MLL1 and DOT1L cooperate with Meningioma-1 to induce AML

Simone S. Riedel, Jessica N. Haladyna, Matthew Bezzant, Brett Stevens, Daniel A. Pollyea, Amit U. Sinha, Scott A. Armstrong, Qi Wei, Roy M. Pollock, Scott R. Daigle, Craig T. Jordan, Patricia Ernst, Tobias Neff and Kathrin M. Bernt

Supplemental Material

Supplemental Figure 1

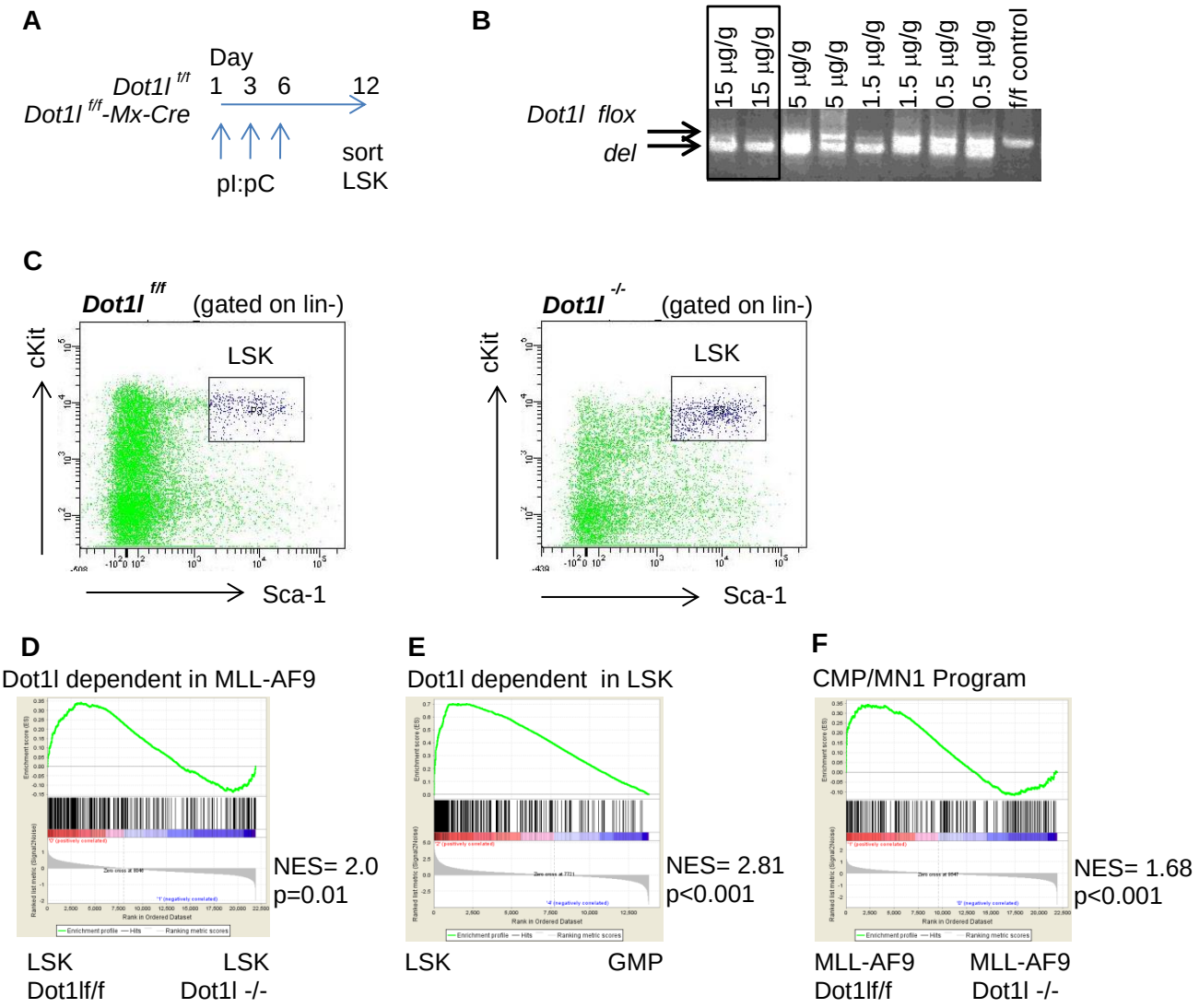

Supplemental Figure 1. Experimental design scheme and representative flow sort to determine Dot1l dependent gene set in LSK cells.

A: Experimental design scheme: *Dot1l*$^{f/f}$ (control) and *Dot1l*$^{f/f}$ *Mx-Cre* mice, 6 mice per group, were injected with 3 doses of pI:pC (15 µg/g mouse weight) on days 1, 3 and 6. Mice were sacrificed on day 12 (6 days after the last injection of pI:pC). LSK cells were sorted for gene expression profiling.

B: Pilot experiment determining pI:pC dose given with the schedule above. Only highest dose of 15 µg/g mouse weight yielded full deletion. Improved deletion with the lower doses could also not be achieved with additional doses (up to 6 total doses for 0.5 and 1.5 µg/g, data not shown).

C: Flow plots for control mice showed the expected pattern with no or minimal residual effects from pI:pC. *Dot1l*$^{-/-}$ mice show a beginning decrease in cKit expression particularly in the progenitor compartment (*cKit* is a Dot1l dependent gene by expression array), but the LSK cells are still clearly identifiable.

D: GSEA showing enrichment of genes dependent on Dot1l in MLL-AF9 driven leukemia ("MLL-AF9 Dot1l-down", defined as genes downregulated in MLL-AF9 driven murine leukemia 7 days after loss of Dot1l at p<0.01, (1)) in *Dot1l*$^{f/f}$ LSK vs *Dot1l*$^{-/-}$ LSK cells. NES/p-value according to (2)

E: GSEA showing enrichment of genes dependent on Dot1l in LSK cells ("LSK Dot1l-down, defined as genes downregulated in LSK cells 6 days after loss of Dot1l at p<0.05) in the set of genes downregulated at the LSK to GMP transition (i.e. up in LSK, down in GMP). NES/p-value according to (2)

F: GSEA showing enrichment of the "CMP/MN1 Program" in *Dot1l*$^{f/f}$ vs *Dot1l*$^{-/-}$ MLL-AF9 leukemias (1). NES/p-value according to (2)

Please also refer to Supplemental Materials and Supplemental Tables 1 (differentially expressed genes LSK *Dot1l*$^{f/f}$ vs LSK *Dot1l*$^{-/-}$) and 2 (gene lists used for GSEA). Supplied as an Excel file.

Supplemental Figure 2

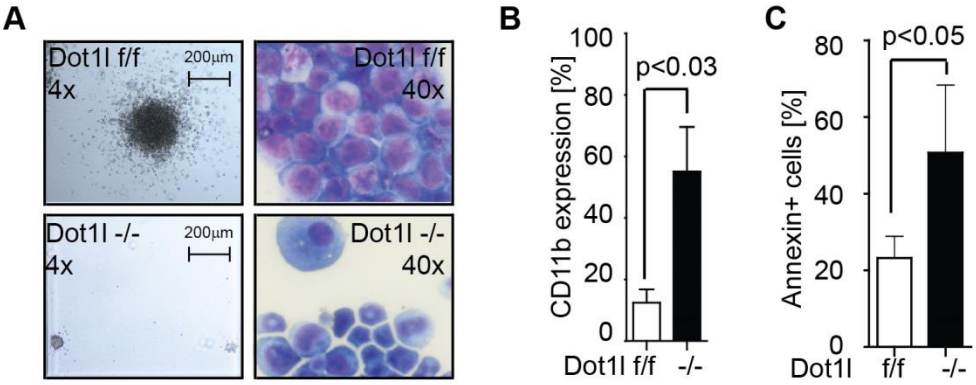

Supplemental Figure 2. Differentiation and apoptosis in ^{MN1}CMP-T.

A: Methylcellulose colony and cell morphology (Wright Giemsa staining) of MN1 transformed CMPs (^{MN1}CMP-T) 27 days after transduction with Cre.

B: CD11b expression in ^{MN1}CMP-T 3 weeks after deletion of *Dot1l*. N=3 independent experiment, 2-sided t-test *Dot1l*$^{-/-}$ vs *Dot1l*$^{f/f}$, error bars: SEM.

C: Apoptosis (Annexin staining) in ^{MN1}CMP-T 3 weeks after deletion of *Dot1l*. N=3 independent experiments, 2-sided t-test *Dot1l*$^{-/-}$ vs *Dot1l*$^{f/f}$, error bars: SEM.

Supplemental Figure 3

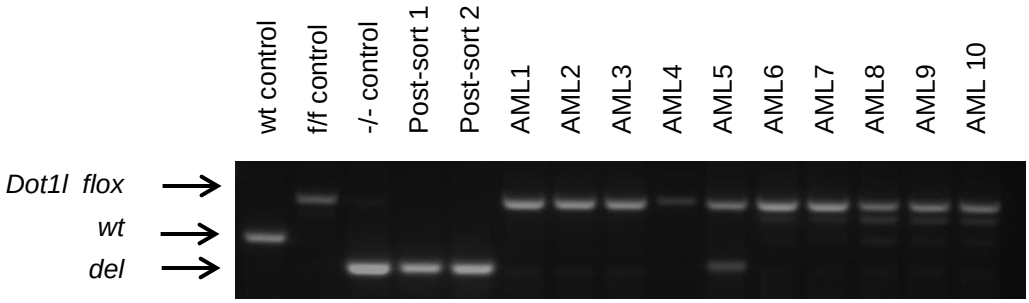

Supplemental Figure 3. Outgrowth of leukemia cells with at least one floxed allele in primary and secondary MN1 driven leukemias (genomic PCR).

Supplemental Figure 4

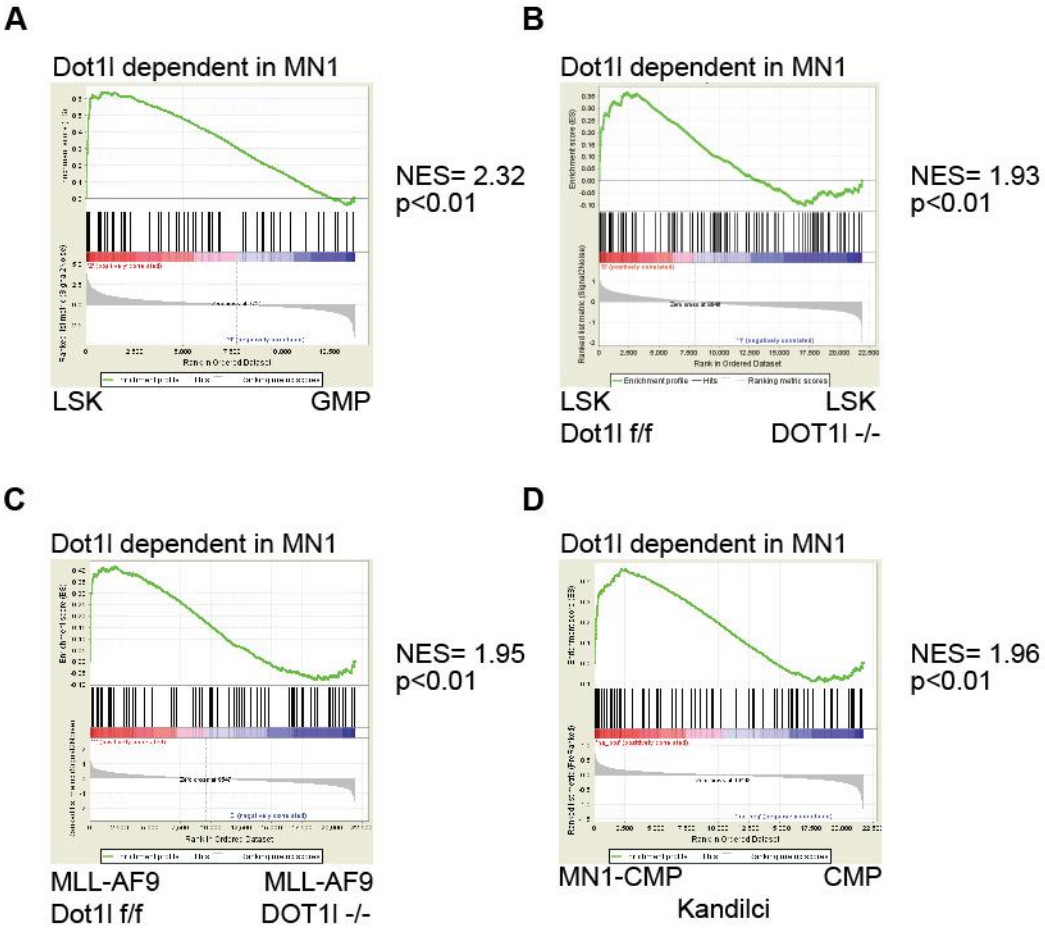

Supplemental Figure 4. Gene set enrichment analysis (GSEA) of genes dependent on Dot1l in ^{MN1}CMP-T ("Dot1l dependent in MN1", defined as top 200 dysregulated genes).

A: GSEA showing enrichment of genes dependent on Dot1l in ^{MN1}CMP-T in genes downregulated at the LSK to GMP transition (3). NES/p-value according to (2).

B: GSEA showing enrichment of genes dependent on Dot1l in ^{MN1}CMP-T in *Dot1l*$^{f/f}$ vs *Dot1l*$^{-/-}$ LSK cells. NES/p-value according to (2).

C: GSEA showing enrichment of genes dependent on Dot1l in ^{MN1}CMP-T in MLL-AF9 *Dot1l*$^{f/f}$ vs *Dot1l*$^{-/-}$ leukemias (1). NES/p-value according to (2).

D: GSEA showing enrichment of genes dependent on Dot1l in ^{MN1}CMP-T in murine MN1-transforemd CMPs vs control CMPs (4). NES/p-value according to (2).

Please also refer to Supplemental Materials and Supplemental Tables 2 (gene lists used for GSEA) and 3 (differentially expressed genes ^{MN1}CMP-T *Dot1l*$^{f/f}$ vs *Dot1l*$^{-/-}$). Supplied as an Excel file.

Supplemental Figure 5 A - E.

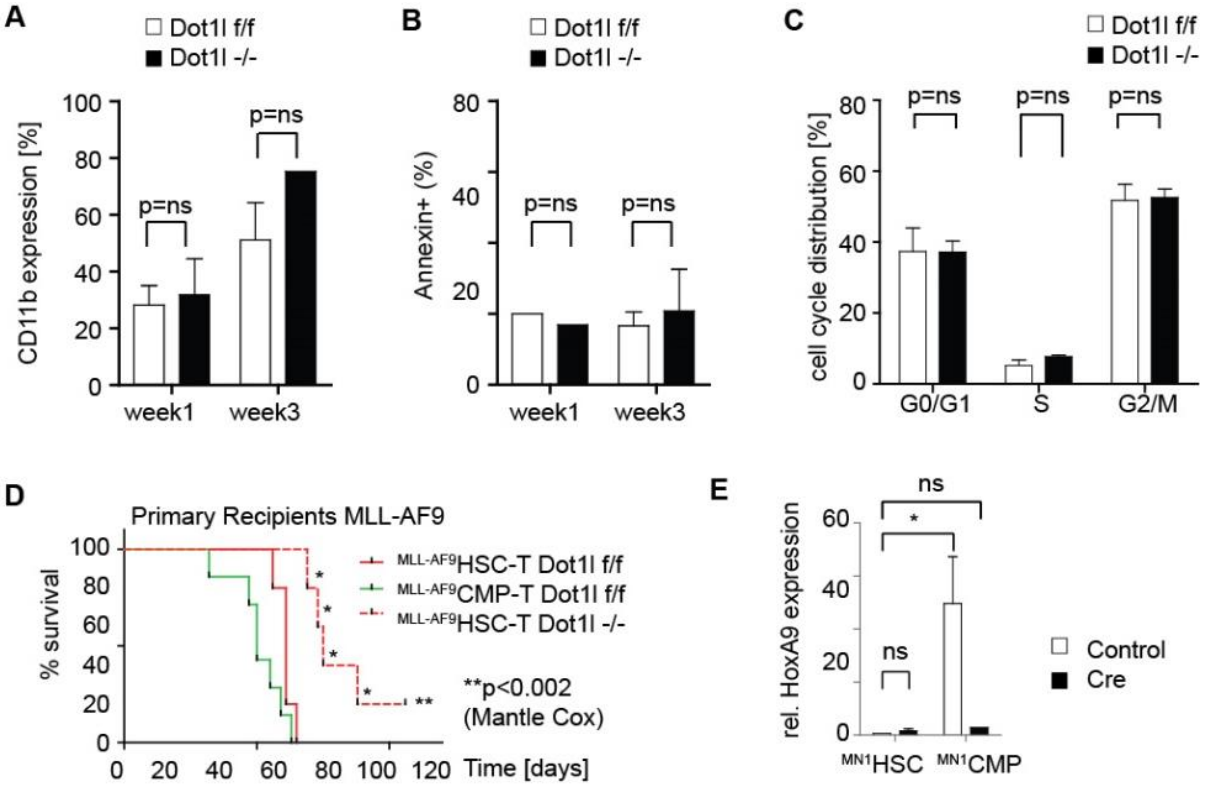

Supplemental Figure 5. ^{MN1}HSC-T grow independently of Dot1l in vitro but not in vivo.

A: CD11b expression in MN1 transformed HSCs 1 and 3 weeks after deletion of *Dot1l.* Bulk population from 3 independent experiments, 2-sided t-test *Dot1l*$^{-/-}$ vs *Dot1l*$^{f/f}$, error bars: SEM. There are no statistically significant differences between *Dot1l*$^{f/f}$ and *Dot1l*$^{-/-}$ ^{MN1}HSC-T (p=ns). Interestingly, CD11b expression increases over time in these cultures, a phenomenon we have not seen to this extent in CMP derived cultures. The significance of this finding is unclear, but could relate to the inferior ability of these cells to cause in vivo leukemias.

B: Apoptosis (Annexin staining) in MN1 transformed HSCs 1 and 3 weeks after deletion of *Dot1l*. Bulk population from 3 independent experiments. 2-sided t-test *Dot1l*$^{-/-}$ vs *Dot1l*$^{f/f}$, error bars: SEM. p= not significant (ns).

C: Cell cycle distribution (EdU incorporation/DAPI staining) in MN1 transformed HSCs 3 weeks after deletion of *Dot1l*. Bulk population from 3 independent experiments. 2-sided t-test *Dot1l*$^{-/-}$ vs *Dot1l*$^{f/f}$, error bars: SEM. p= not significant (ns).

D: Survival of primary recipients of MLL-AF9 in vitro transformed $^{MLL\text{-}AF9}$CMP-T, and $^{MLL\text{-}AF9}$HSC-T transduced with either Cre or control. 100 000 cells/mouse, n=6 ($^{MLL\text{-}AF9}$CMP-T), n=5 ($^{MLL\text{-}AF9}$HSC-T-Cre), and 5 ($^{MLL\text{-}AF9}$HSC-T control), **p<0.02 $^{MLL\text{-}AF9}$HSC-T control vs Cre (Mantel-Cox). *: failure to rearrange both *Dot1l* floxed alleles confirmed by genomic PCR.

E: qPCR for HoxA9 in ^{MN1}CMP-T and ^{MN1}HSC-T, each bar represents fold-change in the indicated population compared to ^{MN1}HSC-T control (set to 1, first bar). Error bars: SEM, *p<0.01, ns: p=not significant (2-sided t-test of indicated population vs ^{MN1}HSC-T control).

Supplemental Figure 5 F - J

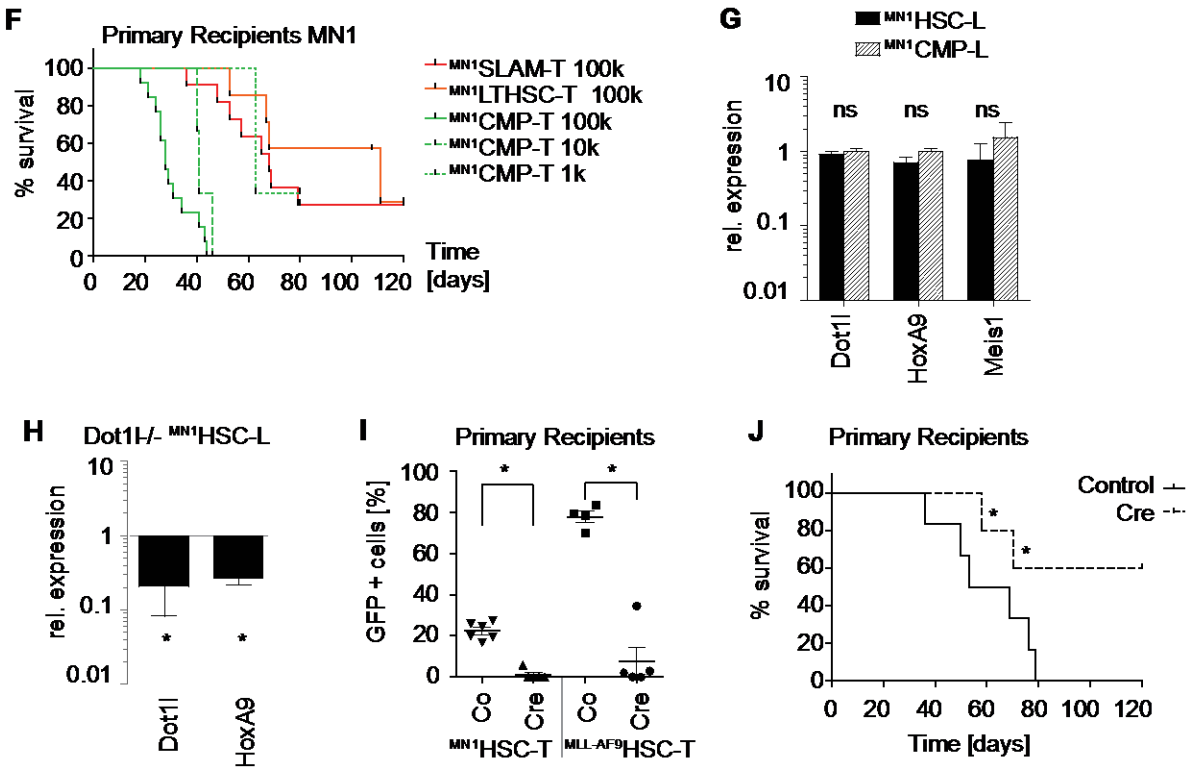

F: Survival of primary recipients of sorted, MN1 in vitro transformed CMPs (^{MN1}CMP-T, including limiting dilution), LSK-SLAM (^{MN1}SLAM-T) and LT-HSCs (^{MN1}LTHSC-T). Of note, MN1 levels in the sorted transduced populations were similar (data not shown). ^{MN1}CMP-T 100k: n=13, 3 individual experiments; ^{MN1}CMP-T 10k: n=3; ^{MN1}CMP-T 1k: n=3; ^{MN1}SLAM-T: n=8, 2 individual experiments; ^{MN1}LTHSC-T: n=7, 2 individual experiments. ^{MN1}CMP-T 100k versus ^{MN1}CMP-T and ^{MN1}SLAM-T: p<0.0001 (Mantel-Cox). Given that the starting populations for HSC transductions were highly enriched for, but not purely comprised of HSCs, we assume that some or all of these leukemias in the HSC group originated from a co-purified early progenitor.

G: qPCR for Dot1l, HoxA9 and Meis1 in "HSC" and CMP derived in vivo leukemias: fold change in ^{MN1}HSC-L relative to ^{MN1}CMP-L (set to 1). N=3, 2-sided t-test, error bars: SEM, ns: p=not significant.

H: qPCR for Dot1l and HoxA9 in ^{MN1}HSC-L ("HSC"-derived in vivo leukemias) 7 days after ex vivo deletion of *Dot1l* (*Dot1l*$^{-/-}$); each bar represents fold-change in *Dot1l*$^{-/-}$ compared to *Dot1l*$^{f/f}$ (set to 1). N=3, error bars: SEM, *****p<0.01 (t-test *Dot1l*$^{-/-}$ vs *Dot1l*$^{f/f}$).

I: Leukemic burden in primary recipients (measured as % GFP+ cells in the peripheral blood) on day 38 after transplantation with 100 000 ^{MN1}HSC-T and $^{MLL-AF9}$HSC-T transduced with either Cre or Control (Co). ^{MN1}HSC-T: n=6 per group, 2 independent experiments; $^{MLL-AF9}$HSC-T: n= 5(Cre) and 4(Co) per group, error bars: SEM, *p<0.001 (2-sided t-test).

J: Survival of primary recipients of 100 000 MN1 in vitro transformed ^{MN1}HSC-T transduced with either Cre or control, n=6 per group, 2 independent experiments, p<0.05 (Mantel-Cox). *: failure to rearrange both *Dot1l* floxed alleles confirmed by genomic PCR.

Supplemental Figure 5 K+L

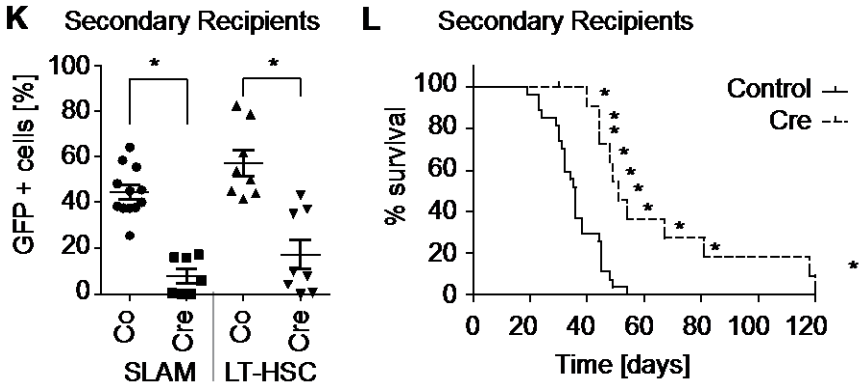

K: Leukemic burden in secondary recipients (measured as % GFP+ cells in the peripheral blood) on day 38 after transplantation with 100 000 ^{MN1}HSC-L (either LT-HSC or LKS-SLAM derived) transduced with either Cre or Control (Co). N = 12 (LSK-SLAM-Control), 7 (LSK-SLAM-Cre), 8 (LT-HSC-Control) and 8 (LT-HSC-Cre) from 3 (LT-HSC) and 2 (LSK-SLAM) primary leukemias, 6 independent experiments; error bars: SEM, *p<0.001 (2-sided t-test).

L: Survival of secondary recipients of 100 000 ^{MN1}HSC-L transduced with either Cre or control, n = 12 (LSK-SLAM-Control), 7 (LSK-SLAM-Cre), 8 (LT-HSC-Control) and 8 (LT-HSC-Cre) from 3 (LT-HSC) and 2 (LSK-SLAM) primary leukemias, 6 independent experiments, **p<0.001 (Mantel-Cox). *: failure to rearrange both *Dot1l* floxed alleles confirmed by genomic PCR.

Supplemental Figure 5 M - P

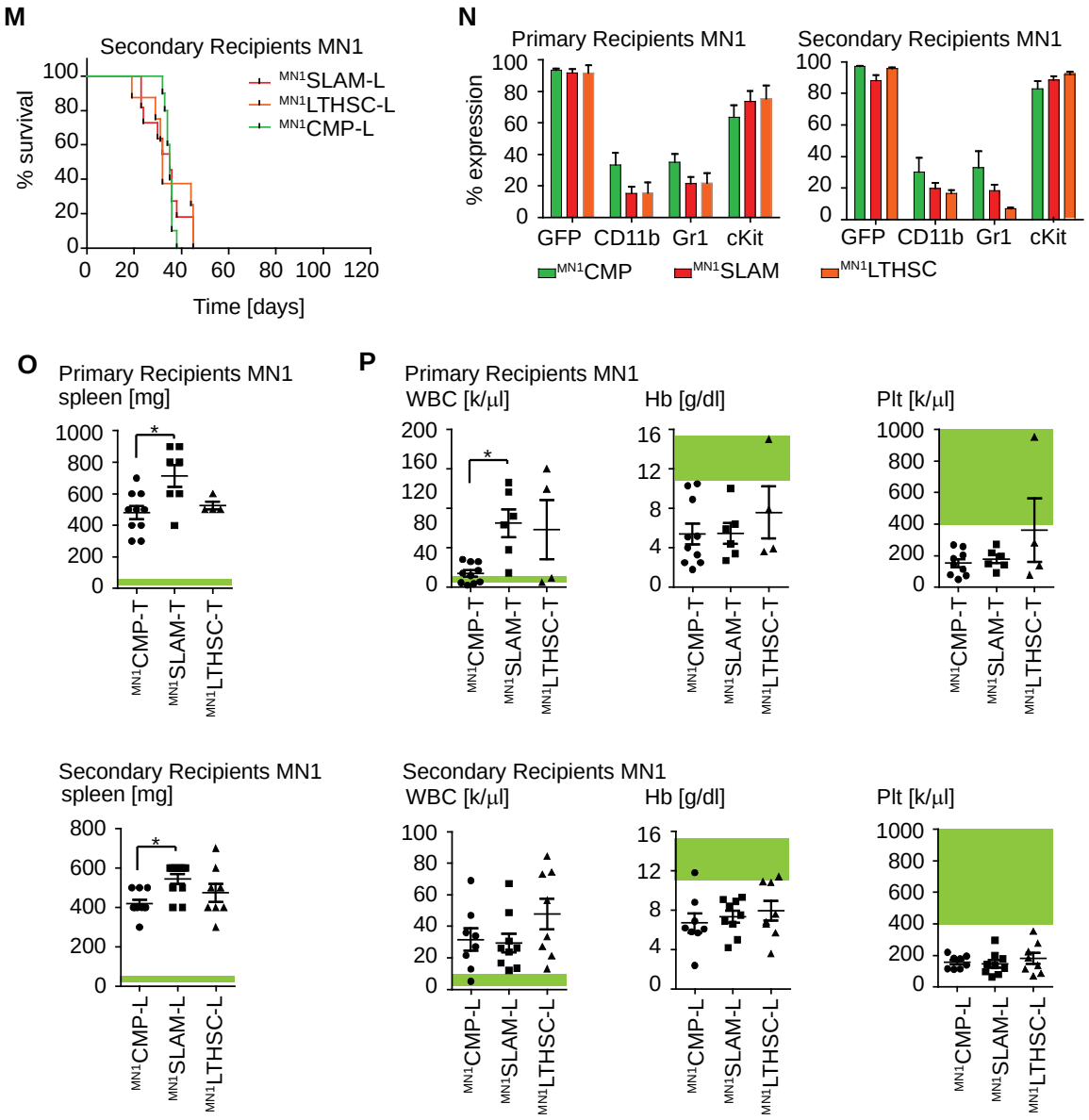

M: Survival of secondary recipients MN1 leukemias based on cell of origin: ^{MN1}CMP-L, n=10), LSK-SLAM (^{MN1}SLAM-L, n=11), and LT-HSCs (^{MN1}LTHSC-L). p = not significant (Mantel-Cox).

N: Flow cytometric analysis of the bone marrow of mice from Supplemental Figure 5G (primary recipients) and N (secondary recipients) at the time of death. Leukemic burden is estimated by the amount of GFP+ cells in the bone marrow.

O: Spleen weight of primary and secondary recipient mice injected with 100,000 ^{MN1}CMP-T, ^{MN1}SLAM-T, or ^{MN1}LT-HSC-T at the time of death. N = 11(^{MN1}CMP-T), 6 (^{MN1}SLAM-T), 3 (^{MN1}LT-HSC-T), 10(^{MN1}CMP-L), 11 (^{MN1}SLAM-L), and 8 (^{MN1}LT-HSC-L).

P: Complete blood count of primary and secondary recipient mice injected with 100,000 ^{MN1}CMP-T, ^{MN1}SLAM-T, or ^{MN1}LT-HSC-T at the time of death. N = 11(^{MN1}CMP-T), 6 (^{MN1}SLAM-T), 3 (^{MN1}LT-HSC-T), 10(^{MN1}CMP-L), 11 (^{MN1}SLAM-L), and 8 (^{MN1}LT-HSC-L). Green shaded area: normal range. **M-P:** Error bars: SEM. *p<0.05 (ANOVA).

Supplemental Figure 6

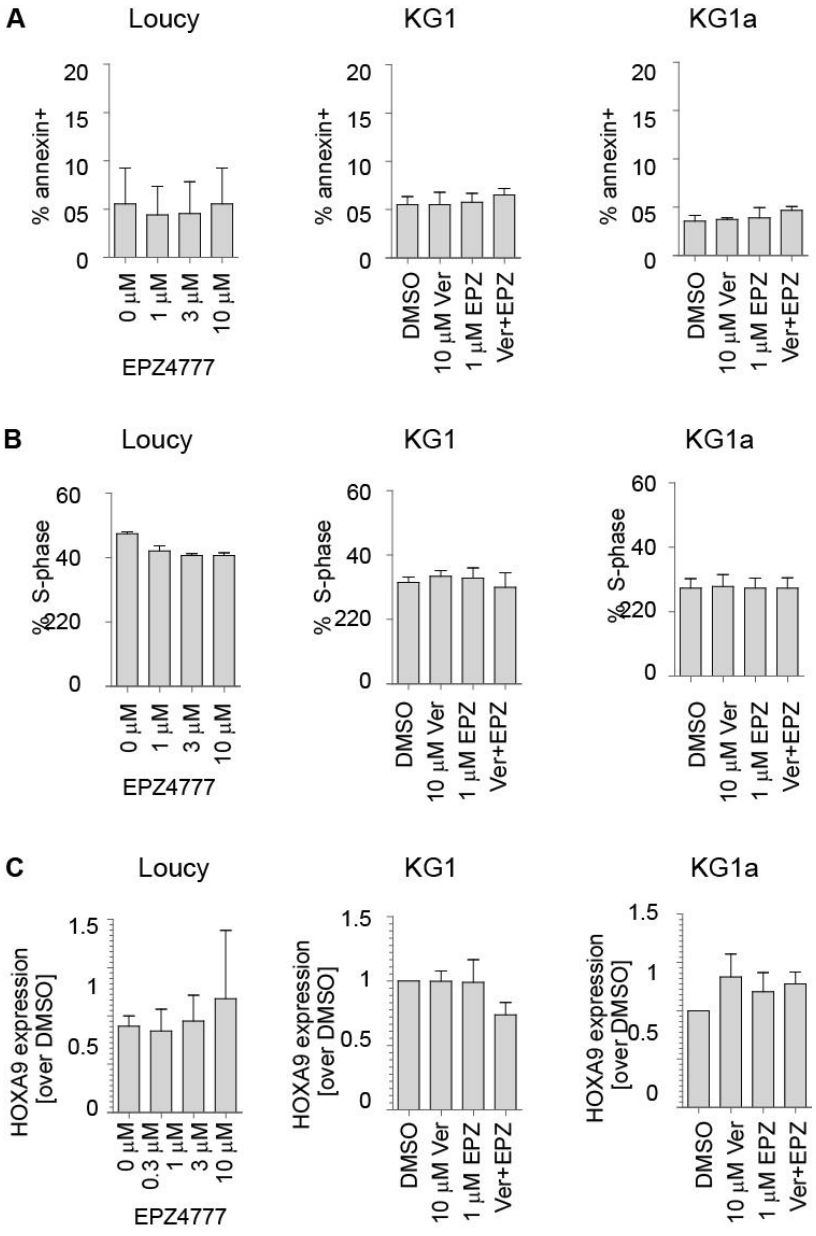

Supplemental Figure 6. Dot1l independence of several HOXA9^{high} cell lines.

Exposure of Loucy, KG1, and KG1a to EPZ4777 (and verapamil) at the indicated concentrations. N=3 independent experiments performed in duplicate, error bars = SEM, p = not significant for all conditions/cell lines, Anova).

A apoptosis (annexin staining); **B** cell cycle (% cells in S-phase, EdU incorporation); **C** HOXA9 expression (qPCR, fold change compared to DMSO set to 1).

Supplemental Figure 7

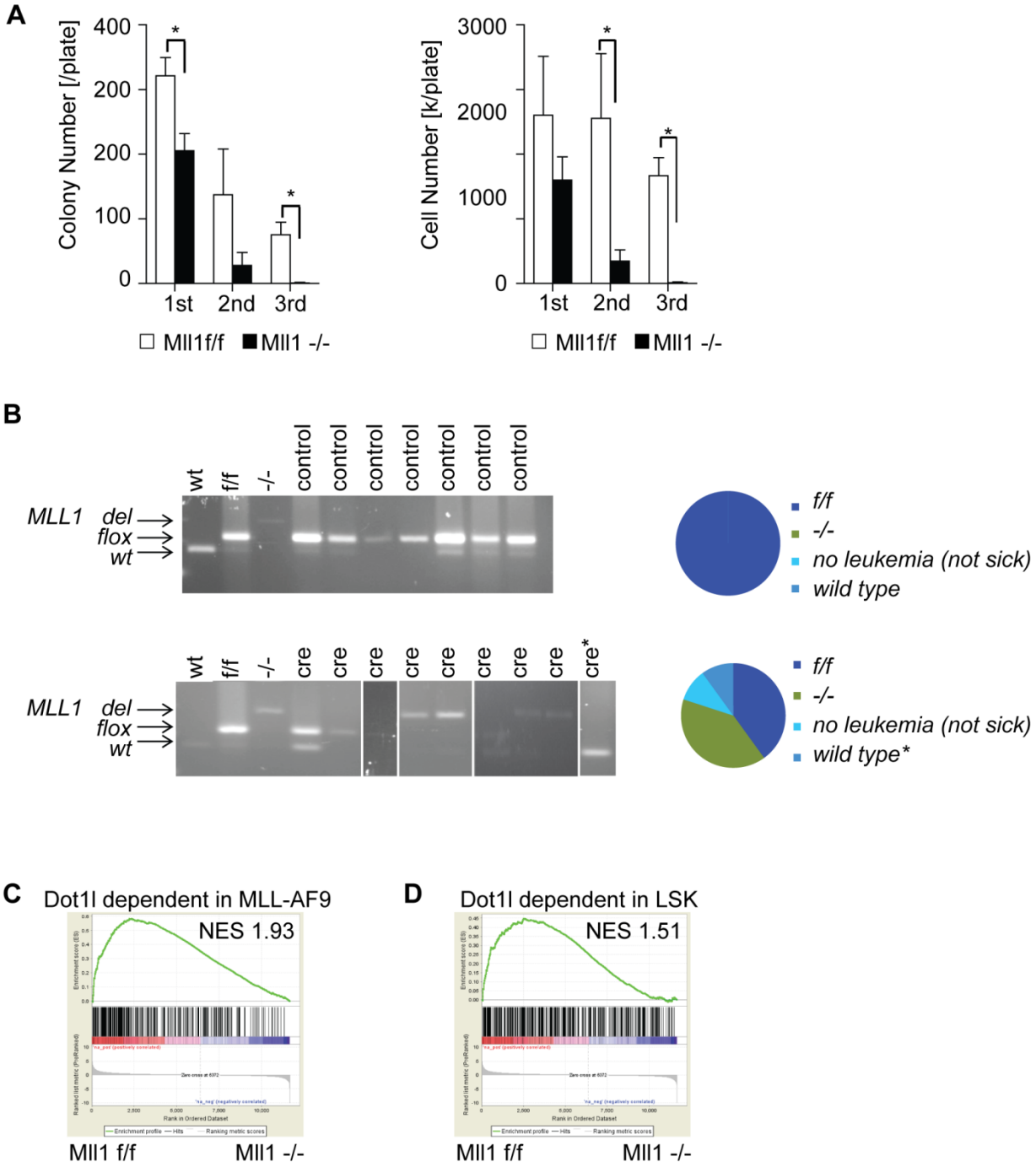

Supplemental Figure 7: Loss of *Mll1* leads to decreased growth of MN1 driven, CMP derived in vitro transformed cells.

A: Serial replating of MN1 transformed CMPs (^{MN1}CMP-T) after Cre-induced loss of *Mll1*. Left plot: number of colonies per 500 plated cells, right plot: total cell number. N= 5 independent experiments, 2-sided t-test in Mll1f/f vs Mll1-/-, error bars: SEM, *p<0.05.

B: Genotyping of bone marrow from secondary recipients transplanted with cre- and control transduced *Mll1*$^{f/f}$ ^{MN1}CMP-L. Lanes are loaded in the order of date of sacrifice/death. As expected, control leukemias had homozygously floxed alleles. 4/10 cre-transduced leukemias show outgrowth of leukemia cells with at least one floxed allele, and these leukemias tended to present earlier (first three cre lanes). 4/10 leukemias show deletion of both copies of *Mll1*. Two animals did not develop leukemia. (*) One animal was found dead 3 months after the end of the experiment, limiting the ability to evaluate the animal, but genomic PCR of the one marrow only revealed only a wild type band consistent with an absence of either *Mll1* deleted or floxed leukemia. One animal was alive at the time of submission (> 6 months after transplant).

Wild type bands in leukemic animals are due to residual normal hematopoiesis and bone marrow stroma from recipient wild type C57BL/6 animals. Genotyping for Cre animals was not run on the same gel, but each gel included a size marked as well as appropriate controls. Individual gels are indicated through dividing lines.

C: GSEA showing enrichment of the “Dot1l dependent in MLL-AF9” program in *Mll1*$^{f/f}$ vs *Mll1*$^{-/-}$ ^{MN1}CMP-L. NES/p-value according to (2).

D: GSEA showing enrichment of the “Dot1l dependent in LSK” program in *Mll1*$^{f/f}$ vs *Mll1*$^{-/-}$ ^{MN1}CMP-L. NES/p-value according to (2).

Supplemental Figure 8 A – D

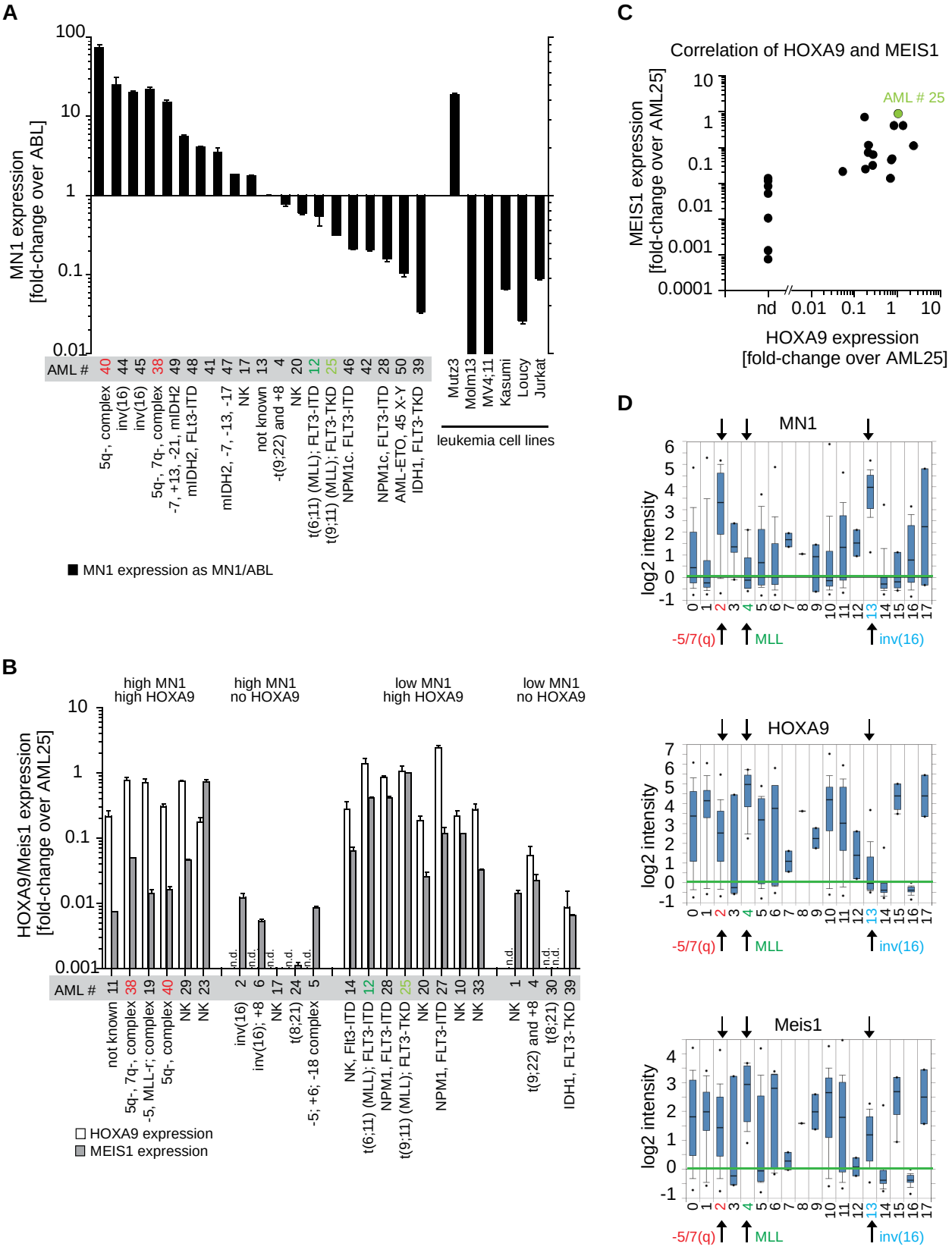

Supplemental Figure 8: A subgroup of MN1high AML patient samples expresses HOXA9 and is sensitive to DOT1L inhibition.

A: qPCR analysis of MN1 in 19 primary patient AML samples and 6 AML cell lines with quantitative ipsogen kit. The graph shows MN1 expression over Abl as determined on a standard curve. Error bars: SD of 2 technical replicates.

B: qPCR analysis of HOXA9 and MEIS1 in 23 primary patient AML samples (not enough material was available to assess MEIS1 expression in AML 34 and 36). HOXA9/MEIS1 expression is plotted as fold-enrichment compared to AML25 (*MLL*-rearranged, with known high HOXA9/MEIS1 expression). Error bars: SEM of 3 technical replicates. nd: not detected.

C: Correlation of HOXA9 and MEIS1 expression in 23 primary patient AML samples.

D: MN1, HOXA9 and MEIS1 expression in "Wouters Leukemia" data set (Oncomine^{TM}). 0: Not determined (90), 1: +8 (20); 2: -5/7(q) (29); 3: -9q (6); 4: 11q23 (10); 5: Complex (13); 6: Failure (12); 7: MDS -7(q) (2); 8: MDS -Y (1); 9: MDS Complex (3); 10: Normal (187); 11: Other (53); 12: abn(3q) (2); 13: idt(16) (34); 14: t(15;17) (21); 15: t(6;9) (6); 16: t(8;21) (35); 17: t(9;22) (2). N=526 AML samples.

Supplemental Figure 8 E + F

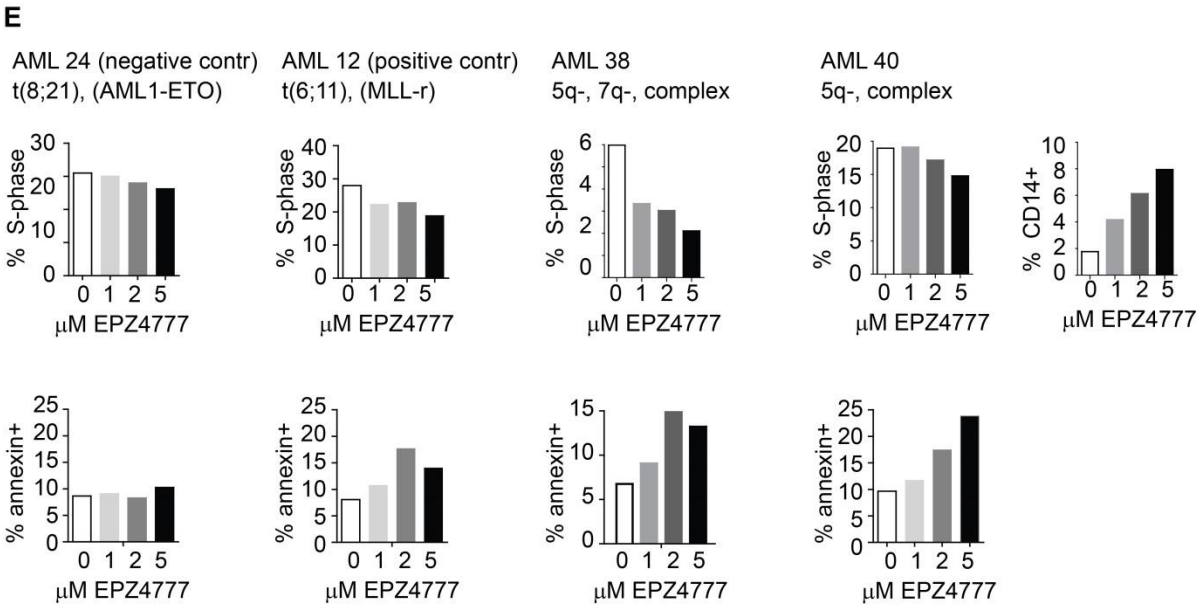

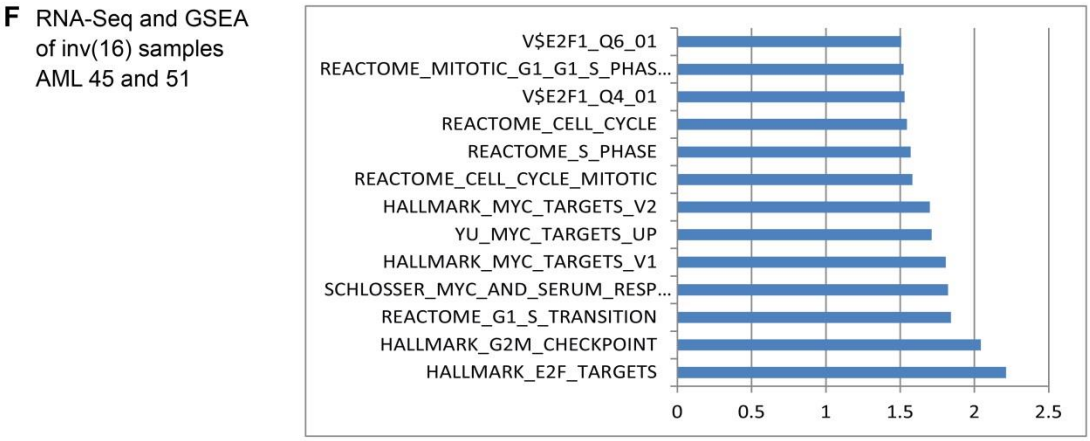

Supplemental Figure 8 E + F

E: Exposure of 4 primary patient AML samples to the DOT1L inhibitor EPZ4777 at the indicated concentrations. Shown is the day 14 flowcytometric analysis for cell cycle (% cells in S-phase, EdU incorporation, top panel), apoptosis (annexin staining, lower panel) and differentiation (CD14 expression by flow cytometry, top right panel).

F: Pathway analysis of inv(16) AML samples treated with 5 µM EPZ4777 for 7 days compared to vehicle control (RNA-Seq).

Supplemental Figure 8 G – H

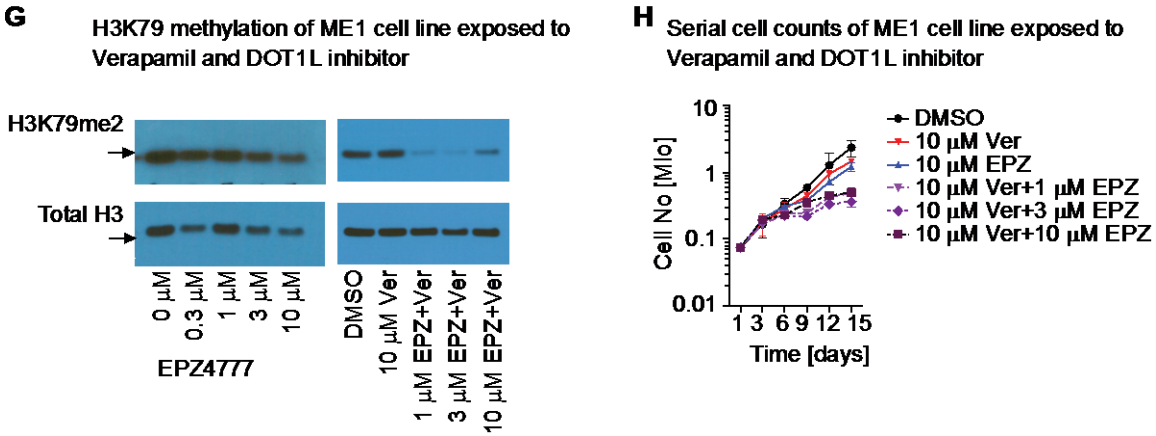

G: ME1 cells require the addition of verapamil to achieve a substantial decrease of H3K79 methylation.

H: Exposure of the inv(16) AML cell line ME1 to EPZ4777 + Verapamil results in decreased growth.

Supplemental Table 4:

#	Age	Gender	Disease	Initial/ Relapse	CYTO	% Blasts	FLT3 ITD	FLT3 TKD	NPM1	IDH	C-KIT
1	67	Female	AML	I	NK	94%	WT	WT			
2	60	Male	AML	I	inv(16)	82%	WT	WT	WT		
4	41	Female	AML from CML	I	t(9;22); +8	26%	WT	WT			
5	65	Male	AML	R	-5; +6; -18; del(20q)	23%					
6	35	Male	AML	R	inv(16); +8;	29%	WT	WT	WT		
10	60	Male	AML	I	NK	93%	WT	WT	WT		
11	59	Female	AML								
12	31	Female	AML	I	t(6;11)	55%	+	WT			
14	58	Female	MDS/AML	I (MDS)*	NK	45%	+	WT	WT		
17	60	Female	AML	I	NK	80%	WT	WT	WT		
19	64	Male	AML	I**	+ 17; -5; -11; 11q23 rearr.; -22	38%	WT	WT			
20	54	Male	AML	I	NK	68%	WT	WT	WT		
23	54	Male	AML	I	NK	29%	WT	WT	WT		
24	48	Female	AML	I	t(8;21)	50%	WT	WT			
25	nd	Male	AML	I	t(9;11)	>80%	weak	+	WT		
27	45	Female	AML	I	NK	75%	+	WT	+		
28	nd	Female	AML	I	NK	>80%	+	WT	+		
29	55	Male	AML	I	NK	38%	WT	WT	WT		
30	35	Male	AML	I	t(8;21)	24%	WT	WT	WT		D816V
33	76	Male	AML	I	NK	65%	WT	WT			
34	78	Male	AML		+8; -17; -21	22%	WT	WT	WT		
36	79	Female	AML	R	Trisomy 8	20%	WT	WT	WT		
38	75	Female	MDS/AML	I (MDS)*	del5q; del7q; -4; -16; -13	76%	WT	WT	WT		
39	nd	nd	AML	I	no data	>80%	WT	D835	WT		
40	nd	Male	AML	I	5q- complex	>80%	WT	WT	WT		
41	38	Male	AML	I	del(16q22)	79%	WT	WT	WT		
42			AML	I							
44	21	Male	AML	I	inv(16)	71%	low	WT	WT		D816V
45	68	Female	AML	I	inv(16)	87%	WT	WT	WT		
46	nd	nd	AML	I	nd	>80%	+	WT	+		
47	nd	Nd	AML	I		>80%					
48	nd	Female	AML	I	t(6;9)	>80%	+	+	WT	IDH2 R140	
49	85	Male	AML	I	XXYY, -7, +13,-21	90%	WT	WT	WT	IDH2 R140	
50	nd	Male	AML	I	X-Y, t(8;21)	>80%					
51	0.6	Female	AML	I	inv(16)	40%	WT	WT			

Supplemental Table 4:

Patient characteristics of newly diagnosed AML patients included in this study. AML samples from patients 25, 28, 39, 40 and 46 were diagnosed at the University of Rochester and kindly provided by Dr. Craig Jordan, no clinical information was available except that this was an initial diagnostic sample, and that blast count was >80%.

nd=no data

* patient with MDS and previous treatment with decitabine (14) or azacytinine (38), sample analyzed is the sample that diagnosed progression to AML

**sample is post-induction chemotherapy with primary refractory disease

Supplemental Experimental Procedures:

Human Samples:

The samples from AML patients were obtained from diagnostic procedures at the University of Colorado Hospital (Protocol 06-0720), with patient informed consent for genetic analysis according to the Declaration of Helsinki, and institutional review board approval from all participating centers. Conventional chromosome banding and fluorescence-in-situ-hybridization (FISH) were performed at the Colorado Genetics Laboratory. Molecular analysis was performed at Children's Hospital Colorado, Department of Pathology.

Cell growth assays and DOT1L inhibition for patient samples

Patient AML samples were plated in media containing TPO, Flt3L, IL3, IL6 and SCF as described by (5). Samples were plated on a small array of feeder cells (OP9, HS27, HS27a, AFT024) to determine optimal growth support. The DOT1L inhibitor EPZ4777 or DMSO control was added at the indicated concentrations. Inhibition of H3K79 methylation was verified by Western Blotting on day 3 or 4. Cells were counted, washed and replated in fresh compound onto fresh feeders at equal densities every 3-4 days for 10-21 days.

Cell Lines

The following human cell lines were obtained from *American Type Culture Collection*: Jurkat, Clone E6-1 (ATCC TIB-152), Loucy (ATCC CRL-2629); KG1 (ATCC CRL-8031), KG1a (ATCC CCL-246.1), and MV-4;11 (ATCC CRL-9591). The following cell lines were purchased from the *Deutsche Sammlung von Mikroorganismen und Zellkulturen* (DSMZ, Germany): MOLM-14 (DMSZ ACC 554) Me1 (DMSZ ACC 537) and Mutz3 (DMSZ ACC 295). KG1, KG1a, Loucy, MV4;11, Molm14, Me1 and Jurkat cells were maintained in RPMI-1640 media (Corning) supplemented with heat-inactivated 10% fetal bovine serum, 2 mM L-glutamine and 50 U/ml Penicillin/Streptomycin (all Life Technologies, Grand Island, NY). Mutz3 cells were maintained in α–MEM (Hyclone, Logan, UT), supplemented with heat-inactivated 20% fetal bovine serum,

2 mM L-glutamine, 50 U/ml Penicillin/Streptomycin and 40 ng/ul GM-CSF (Peprotec, Rocky Hill, NJ). All cells were cultured in the appropriate medium in a humidified incubator at 37°C in 5% CO2. DOT1L inhibitor assays were performed as described for the primary human samples, but without feeders.

Genomic PCR and primers

Dot1l genotyping was performed using primers p2 (CCCAAAAGGGTCTTTTCACA, forward) and p4 (CACAGAGCCATGACCAGACA, reverse). Excision is confirmed using primers p1 (CTCACAGTCACATACTACCTCTGAC, forward) and p3 (ATGGGATTTCATGGAAGCAA, reverse) for the excised allele, and p2 and p3 for the floxed allele. *MLL* genotyping was performed using primer sequences forward: tct ctg aag taa gcc ttt ctt ag, reverse 1: cag tgg aca ttc caa ctc ttc aa and reverse 2: cac cca gca ttg cag agt cag.

***Dot1l* and *Mll1* knockout mice, breeding, pI:pC injections**

Animals were maintained at the Animal Research Facility at the University of Colorado Anschutz Medical Campus. Animal experiments were approved by the Internal Animal Care and Use Committee. *Dot1l* (1) and *Mll1* (6) conditional knockout mice were previously described and were maintained on a fully backcrossed C57BL/6 background. *Dot1l* conditional knockout mice were also crossed with *Mx1Cre* mice to yield and *Dot1l*$^{f/f}$ *Mx-Cre* mice. To induce in vivo *Dot1l* deletion, mice were injected i.p. with pI:pC (15 μg/g mouse weight) on days 1,3 and 6.

Generation of MN-1 leukemias

The *MN-1* cDNA was generously provided by Ellen C. Zwarthoff (Erasmus University Rotterdam, Netherlands) and re-cloned into an MSCV based vector (MIG, MSCV-IRES-GFP) followed by IRES-GFP cassette (MN1-GFP). The MSCV-based Cre-IRES-pTomato (cre) and MSCV-IRES-pTomato (control) or MSCV-based Cre-IRES-trCD2 (Cre) and MSCV-IRES-CD2 (control) were cloned by inserting the cDNA or either pTomato or truncated human CD2 in place of GFP in MIG. Ecotropic retroviral vectors MN-1-IRES-GFP, Cre-IRES-pTomato, Cre-IRES-trCD2, MSCV-IRES-pTomato or MSCV-IRES-CD2 were generated by cotransfection of 293T

cells using FuGENE6 (Roche Molecular Biochemicals, Indianapolis, IN). Virus containing supernatant medium was collected on days 2 and 3 days after the transfection. Wild type, *Dot1l*$^{f/f}$ or *Mll1*$^{f/f}$ donor mice were 3-6 month old male or female. Bone marrow cell suspensions were prepared by crushing bones in a mortar after removal of muscle and connective tissues. Red blood cells were lysed on ice using red blood cells lysis buffer Pharm Lyse (BD Biosciences). Lineage depletion was performed by labeling bone marrow cell suspensions with a mixture of purified biotinylated monoclonal antibodies to CD3e (17A2), CD4 (GK1.5), CD8a (53.6.7), CD19 (1D3), B220 (RA3.6B2), Gr-1 (RB6.8C5), IL-7R (A7R34) and Ter-119 (eBioscience, SanDiego, CA). Lin+ cells were partially removed by 2 rounds of magnetic bead depletion with streptavidin conjugated Dynabeads (Dynal, Life Technologies, Carlsbad, CA). SLAM, LT-HSC, LSK or CMP cells were prepared by staining lineage depleted (lin$^-$) cells with APC-Cy7 conjugated streptavidin (Molecular Probes, Life Technologies, Carlsbad, CA) and stained with combinations of, c-Kit Alexa 647 (clone 2B8), CD48 Pacific Blue (clone HM48-1), CD150 PE (SLAM, clone TC15-12F12.2), CD135 PE (Flk2, clone A2F10), CD16/32 PE **(**FcγRII, clone 93) all BioLegend (San Diego, CA), CD34 FITC (clone RAM34) BD Pharmingen (San Jose, CA), Sca-1 PE-Cy7 (clone D7) eBioscience (Affymetrix, San Diego, CA), and sorted for Lin$^-$Sca-1$^+$c-Kit$^+$ CD48$^-$CD150$^+$ (SLAM), Lin$^-$Sca-1$^+$c-Kit$^+$CD34$^-$CD135$^-$ (LT-HSC), Lin$^-$Sca-1$^+$c-Kit$^+$ (LSK) or Lin$^-$Sca-1$^-$c-Kit$^+$CD34$^+$CD32^{low} (CMP). Sorted cells were pre-stimulated for 24 h with 10 ng/ml mIL3 and mIL6 and 20 ng/ml mSCF, mFlt3L and TPO (Peprotec, Rocky Hill, NJ). Transduction was carried out on retronectin (Takara, Madison, WI) with MN1-GFP in the presence of murine IL3, IL6, SCF, Flt3L and TPO in concentrations as above. Cells were subsequently maintained in M3234 (Stem cell technologies, Vancouver, BC) methylcellulose with 10 ng/ml IL3 and IL6, 20 ng/ml SCF, and 50 U/ml Penicillin/Streptomycin (Gibco, Life Technologies, Carlsbad, CA)**.**

After 4-6 days, GFP-expressing cells (^{MN1}CMP-T or ^{MN1}HSC-T) were sorted and either transplanted into mice, or transduced with Cre or control vector as described above. Four days

after transduction, $GFP^+/pTomato^+$ or $GFP^+/CD2^+$ cells were sorted and transplanted into mice. Transplants were performed into 6 week old C57BL/6 female irradiated (750 RAD) recipients at $1x10^5$ cells/mouse. $1x10^5$ cells/mouse of normal bone marrow were co-transplanted for early support. For secondary transplants, whole bone marrow from moribund leukemic mice was isolated, GFP^+ cells were sorted (yielding ^{MN1}CMP-L or ^{MN1}HSC-L) and blast colonies were allowed to grow out in M3234 for 2-4 days as described above. Leukemic cells were transduced with C

re or control vector, sorted and transplanted as described above. Cell sorting was performed on a Beckman-Coulter MoFlo XDP70, MoFlo AstriosEQ or Beckton-Dickinson AriaII cell sorter.

Biochemical Assays (cell growth, apoptosis, cell cycle analysis, western blotting, qPCR)

Cell growth and viability were followed by serial cell counts and trypan blue exclusion staining**.** For colony assays, sorted transduced cells were plated in methylcellulose M3234 containing 10 ng/ml IL3 and IL6, and and 20 ng/ml SCF at a concentration of 1000 or 5000 cells per plate, and replated at 1000 cells/plate every 6-7 days. For liquid culture, cells were maintained in media containing IL3, IL6 and SCF, and counted and replated at equal densities every 3-4 days.

For the Annexin V apoptosis assay, $1x10^6$ cells were washed in PBS, resuspended in Ca/HEPES buffer (10 mM HEPES, pH7.4; 140 mM NaCl; 2.5 mM CaCl2) and incubated with Annexin V-APC (BD Pharmingen, San Jose, CA**)** for 30 min. DAPI (Molecular Probes, Life Technologies, Carlsbad, CA) was added prior to analysis.

Cell cycle analysis was performed after EdU labeling for 30 minutes using the EdU-Alexa647 kit from Molecular Probes (Life Technologies, Carlsbad, CA) according to the manufacturer's instructions and DAPI added prior to analysis. Data was acquired on a Beckton-Dickinson Gallios 561 cytometer and analyzed using Kaluza^{TM} (Beckton-Dickinson).

For western blotting, we extracted histones (triton extraction (PBS 0.5% TritonX100 (v/v), 2mM phenylmethylsulfonylfluoride, 0.02% (w/v) NaN3 acid extraction) followed by acid extraction with 0.2N HCl). Proteins were separated on a 10% Bis-Tris gel (Nupage, Life Technologies,

Carlsbad, CA) and blotted on nitrocellulose membranes (Novex, Life Technologies, Carlsbad, CA). The following antibodies were used for detection: H3K79me2 rabbit polyclonal abcam (Cambridge, MA) 3594-100, total H3 rabbit polyclonal abcam 1791; secondary antibody for detection: donkey anti rabbit ECL horseradish peroxidase linked NA934V, GE healthcare UK limited (Little Chalfont Buckinghamshire, UK). Proteins were visualized using Western Lightning Plus-ECL (Perkin-Elmer).

For reverse transcription and quantitative PCR, total RNA was isolated using Trizol (Life Technologies, Carlsbad, CA) or RNeasy mini or micro kit (Qiagen, Hilden, Germany) according to the manufacturer's instruction. Resultant cDNA was generated using the tetro cDNA synthesis kit (Bioline, Taunton, MA).

Human cell line qPCR was performed using SYBR green with GPADH and HPRT1 as housekeeping genes. Primer sequences: huGAPDH_qPCR_F: AGCCACATCGCTCAGACA; huGAPDH_qPCR_R: GCCCAATACGACCAAATCC; huHPRT1F: GTGAAAAGGACCCCACGAAG; huHPRT1R: AGGCTTTGTATTTTGCTTTTCCA; huMN1_qPCR_F: GACTCGCTGGAATACAATTACCC; huMN1_qPCR_R: ACCCGCTGCATAATGAGGC; huHOXA9_qPCR_F: CTGTCCCACGCTTGACACTC; huHOXA9_qPCR_R: CTCCGCCGCTCTCATTCTC. GAPDH and HPRT gave highly similar results for all cell lines / assays except the KG1 and KG1a cell lines, where similar cell numbers resulted in similar HPTR, but higher GAPDH cycle numbers, therefore only HPRT was used as housekeeping gene for these two cell lines.

For patient and murine samples, real time PCR was performed using TaqMan detection reagents (TaqMan Gene Expression Master Mix, Applied Biosystems) on the StepOnePlus Real-Time PCR System (Applied Biosystems) using TaqMan probes (all Life Technologies) for HoxA9 (Mm00439364_m1), Meis1a (Mm00487664_m1) and MN1 (Hs00159202_m1). The data were normalized to GAPDH (Mm99999915_g1), and are presented as fold change with respect to cells transduced with vector control. Absolute quantification of MN1 was performed using the

Ipsogen MN1 kit according to the manufacturer's instructions (Qiagen, Hilden, Germany). All experiments were performed with three (Taqman) technical replicates from three to four individual experiments. qPCR analysis of human samples was performed in technical duplicate (Ipsogen) or triplicate (Taqman).

RNA amplification and gene expression array

RNA was isolated from $2x10^4$ sorted *Dot1l*$^{f/f}$ or *Dot* $^{-/-}$ LSK or GMP cells from 6 individual mice using Trizol (Invitrogen, Carlsbad, CA). RNA was amplified using the Nugen Ovation Pico WTA system (Nugen, San Carlos, CA), and labeled using the Nugen Encore^{TM} Biotin Module. 5 µg of amplified and labeled DNA was hybridized to Affymetrix 430 2.A murine microarrays.

Chromatin immunoprecipitation (ChIP)

Chromatin immunoprecipitation for H3K79me2 in murine MN1 leukemias and human cell lines was performed using rabbit polyclonal antibodies from abcam (ab3594 Cambridge, MA) similarly as described (7). Briefly, cells were fixed in PBS 1% formalin (v/v) with gentle rotation for 10 minutes at room temperature. Fixation was stopped by the addition of glycine (125 mM final concentration). Fixed cells were washed twice in ice-cold PBS, resuspended in SDS lysis buffer (1% SDS, 10mM EDTA, 50 mM Tris-HCl, pH 8.1). Chromatin was sheared by sonication to about 100-300bp fragments using EpiShear (Active Motive, Carlsbad, CA) and diluted ten fold with dilution buffer (0.01% SDS, 1.1% Triton-X100, 1.2 mM EDTA, 16.7 mM Tris-HCl, pH 8.1,167 mM NaCl). Magnetic bead labeled antibodies against specific histone modifications were used to precipitate DNA fragments associated with modified histones. Precipitates were washed sequentially with ice cold low salt wash (1% SDS, 1% Triton-X-100, 2mM EDTA, 20mM Tris-HCl, pH8.1, 150mM NaCl), high salt wash (1% SDS, 1% Triton-X-100, 2mM EDTA, 20mM Tris-HCl, pH 8.1, 500mM NaCl), LiCl wash (0.25M LiCl, 1% IGEPAL CA-630, 1% deoxycholic acid, 1mM EDTA, 10mM Tris-HCl, pH 8.1) and TE wash (1mM EDTA, 10mM Tris-HCl, pH 8.1) and eluted in elution buffer (1% SDS, 0.1 M NaHCO3). All buffers except for elution buffer were supplemented with protease inhibitor (Complete mini protease inhibitor cocktail tablets, Roche,

Indianapolis, IN). Eluted DNA fragments were analyzed by bioanalyzer for overall quality in addition to quantitative PCR quality control for known targets/controls using promoter specific primers for HoxA7 (forward: CTCTTCTGTTTCCCATCCTGGT; reverse: GGCAATATCCGGGATCCACT), HoxA9 (forward: GGAATAGGAGGAAAAAACAGAAGAGG; reverse: TGTATGAACCGCTCTGGTATCCTT), HoxA10 (forward: CCTTTTTGGTCGACTCGCTC; reverse: CAACACCAGCCTCGCCTCT), Meis1a (forward: TCACCACGTTGACAACCTCG; reverse: GCTTTCTGCCACTCCAGCTG), HoxB1 (forward: GGGACTGCCAAACTCTGGC; reverse: CATGTGATCTCTCCCAGGCC) and Actin (forward: GGGAACCAGACGCTACGATC; reverse: TTGGACAAAGACCCAGAGGC).

ChIP DNA libraries were made following Illumina ChIP-seq library preparation kit and subjected to sequencing as below (Illumina).

RNA- and CHIP sequencing

RNA was isolated from sorted GFP^{+}/$pTomato^{+}$ cells using Trizol (Invitrogen) followed by column purification with the RNeasy mini or micro kit (Qiagen, Hilden, Germany). cDNA libraries were constructed for each sample (3 Cre, 3 MIT) using the Illumina TruSeq Stranded mRNA sample preparation kit (Illumina, San Diego, CA). The six independently and uniquely indexed libraries were pooled and loaded onto a single lane of a HiSeq2000 flowcell for single-end, 50-bp DNA sequencing using an Illumina HiSeq2000.

Data analysis and statistical methods.

Microarray data analysis: cel files were combined into a gct expression file using GenePattern (Reich et al., 2006), normalizing the raw microarray data using RMA algorithm. LSK *Dot1l*$^{f/f}$ vs *Dot1l*$^{-/-}$ were extracted from the gct file. The gct file was preprocessed using default parameters (PreprocessDataset version 5). Comparative Marker Analysis (version 10) using default parameters except 0 permutations was used to find differentially expressed probe sets, yielding 463 differentially expressed probe sets corresponding to 393 differentially expressed genes.

RNA-Seq analysis: NextGen RNAseq of eleven cDNA libraries (3 Dot1l f/f, 3 Dot1l-/-, 3 MLL1 f/f, 2 MLL1 -/-) yielded 29.2 to 76.8 million total reads per sample. Removal of low-quality bases [Phred score <15] using a custom Python script reduced total sequence data by ≤4%. The remaining sequences were mapped to the annotated mm9 genome (Dumas; NCBI NC_001348) using GSNAP 2012-07-20. Gene expression was calculated using CUFFLINKS Version 2.1 (*Dot1l$^{f/f}$ vs Dot1l$^{-/-}$*) and 2.2.1 (*Mll1$^{f/f}$ vs MLL1$^{-/-}$*). After strand alignment of mm9 sequences, the fragments per kilobase of exon per million mapped reads was determined. Differential gene expression determined using ANOVA, graphic representation at p<0.01 is shown as a heat map.

ChIP-Seq analysis: For Genes associated with K79me2, ChIP-Seq reads and Input reads (used as control) for 3 independent CMP-derived MN1-leukemias were each combined into a single Bam file. MACS2 was used to identify peaks using the parameters --broad -g mm --broad-cutoff 0.1. The resulting peaks were intersected with mm9 Refseq genes using Bedtools (intersectBed). For Genes associated with MN1 peaks, published MN1-peaks from (Heuser et al) were intersected with mm9 Refseq genes using Bedtools (intersectBed). Peaks were visualized using Integrated Genome Viewer (IGV).

Venn Diagrams were generated using Biovenn.

GSEA: Gene set enrichment analysis (GSEA) was performed using (www.broadinstitute.org/gsea *)(2).* To create the "Dot1l-dependent in MN1" signature, the log2-ranked gene list was created. Genes with expression of <0.5 were excluded, genes with expression of 0 in one sample and <5 in the other samples were also excluded. The "Dot1l dependent in MN1" signature was determined as the top 200 differentially expressed genes, after filtering and removal of low quality reads, mirs, snors and contig sequences. To define the CMP/MN1 signature, Gct-files from (8) were collapsed to symbols using the Max_probe mode and genes were ranked on Log2(CMP/GMP) or Log2(MN1/Gr1). The overlap of the top 1000 genes (197 genes) was used as the input geneset for GSEA (Figure 1C, Supplemental Figure 1F, Figure 3C, Figure 7F). The

"Dot1l dependent in MLL-AF9" signature was created using the data set reported in (1). Data was reprocessed using Gene Pattern with default parameters, comparative marker selection was performed with 0 permutations, and the The "Dot1l dependent in MLL-AF9" signature was defined as $p<0.05$ (Supplemental Figure 1D). The "Dot1l dependent in LSK" signature was defined as $p<0.05$ (Supplemental Figure 1E). All four gene sets are available in Supplemental Table 2. In addition, curated list of genesets from MSigdb (Myc/E2F/Proliferation associated datasets) were also used for GSEA (Table 1).

Supplemental References

1. Bernt, K.M., Zhu, N., Sinha, A.U., Vempati, S., Faber, J., Krivtsov, A.V., Feng, Z., Punt, N., Daigle, A., Bullinger, L., et al. 2011. MLL-rearranged leukemia is dependent on aberrant H3K79 methylation by DOT1L. *Cancer Cell* 20:66-78.
2. Subramanian, A., Tamayo, P., Mootha, V.K., Mukherjee, S., Ebert, B.L., Gillette, M.A., Paulovich, A., Pomeroy, S.L., Golub, T.R., Lander, E.S., et al. 2005. Gene set enrichment analysis: a knowledge-based approach for interpreting genome-wide expression profiles. *Proc Natl Acad Sci U S A* 102:15545-15550.
3. Krivtsov, A.V., Twomey, D., Feng, Z., Stubbs, M.C., Wang, Y., Faber, J., Levine, J.E., Wang, J., Hahn, W.C., Gilliland, D.G., et al. 2006. Transformation from committed progenitor to leukaemia stem cell initiated by MLL-AF9. *Nature* 442:818-822.
4. Kandilci, A., Surtel, J., Janke, L., Neale, G., Terranova, S., and Grosveld, G.C. 2013. Mapping of MN1 sequences necessary for myeloid transformation. *PLoS One* 8:e61706.
5. Klco, J.M., Spencer, D.H., Lamprecht, T.L., Sarkaria, S.M., Wylie, T., Magrini, V., Hundal, J., Walker, J., Varghese, N., Erdmann-Gilmore, P., et al. 2013. Genomic impact of transient low-dose decitabine treatment on primary AML cells. *Blood* 121:1633-1643.
6. Artinger, E.L., Mishra, B.P., Zaffuto, K.M., Li, B.E., Chung, E.K., Moore, A.W., Chen, Y., Cheng, C., and Ernst, P. 2013. An MLL-dependent network sustains hematopoiesis. *Proc Natl Acad Sci U S A* 110:12000-12005.
7. Krivtsov, A.V., Feng, Z., Lemieux, M.E., Faber, J., Vempati, S., Sinha, A.U., Xia, X., Jesneck, J., Bracken, A.P., Silverman, L.B., et al. 2008. H3K79 methylation profiles define murine and human MLL-AF4 leukemias. *Cancer Cell* 14:355-368.
8. Heuser, M., Yun, H., Berg, T., Yung, E., Argiropoulos, B., Kuchenbauer, F., Park, G., Hamwi, I., Palmqvist, L., Lai, C.K., et al. 2011. Cell of origin in AML: susceptibility to MN1-induced transformation is regulated by the MEIS1/AbdB-like HOX protein complex. *Cancer Cell* 20:39-52.